

# Optimized pharmacological control over the AAV-Gene-Switch vector for regulable gene therapy

Shi Cheng,<sup>1,3</sup> Marcel M. van Gaalen,<sup>2,4</sup> Mathias Bähr,<sup>1</sup> Enrique Garea-Rodriguez,<sup>2</sup> and Sebastian Kügler<sup>1</sup>

<sup>1</sup>University Medical Center Göttingen, Department of Neurology, Waldweg 33, 37073 Göttingen, Germany; <sup>2</sup>Charles River Laboratories Germany GmbH, Hans-Adolf-Krebs-Weg 9, 37077 Göttingen, Germany

**Gene therapy in its current design is an irreversible process. It cannot be stopped in case of unwanted side effects, nor can expression levels of therapeutics be adjusted to individual patient's needs. Thus, the Gene-Switch (GS) system for pharmacologically regulable neurotrophic factor expression was established for treatment of parkinsonian patients. Mifepristone, the synthetic steroid used to control transgene expression of the GS vector, is an approved clinical drug. However, pharmacokinetics and -dynamics of mifepristone vary considerably between different experimental animal species and depend on age and gender. In humans, but not in any other species, mifepristone binds to a high-affinity plasma carrier protein. We now demonstrate that the formulation of mifepristone can have robust impact on its ability to activate the GS system. Furthermore, we show that a pharmacological booster, ritonavir (Rtv), robustly enhances the pharmacological effect of mifepristone, and allows it to overcome gender- and species-specific pharmacokinetic and -dynamic issues. Most importantly, we demonstrate that the GS vector can be efficiently controlled by mifepristone in the presence of its human plasma carrier protein,  $\alpha$ 1-acid glycoprotein, in a "humanized" rat model. Thus, we have substantially improved the applicability of the GS vector toward therapeutic use in patients.**

## INTRODUCTION

Tight control over expression of neurotrophic factors, as treatments for devastating neurological conditions such as Parkinson's disease (PD) and Alzheimer's disease, can be considered essential to their clinical success: pharmacologically controlled gene therapy may allow us to enroll patients with much less advanced pathology into clinical trials, allowing us to revert neurodegenerative conditions at times where restoration is still possible.<sup>1</sup> Furthermore, transduction of larger brain areas may become possible without having to fear side effects as they have been reported for continuous expression of neurotrophic factor GDNF,<sup>2,3</sup> and intermitted expression of neurotrophic factors may prevent saturation effects of receptors and signaling pathways, thus allowing for better therapeutic efficacy.<sup>4</sup> Several regulable gene therapy systems have been developed, which allow us to place transgene expression under control of a pharmacological compound. However, none of these has reached clinical applicability yet.<sup>5</sup>

The Gene-Switch (GS) regulated system, controlled by the synthetic steroid mifepristone (Mfp), consists mainly of human peptides fused together in the GS protein:<sup>6–10</sup> (1) a truncated human progesterone receptor that does not bind progesterone but Mfp, (2) a transcriptional activation domain from human p65 of the NF- $\kappa$ B complex, and (3) a short peptide of the yeast Gal4-DNA binding domain. Mfp mediates dimerization of the GS protein, which then binds to Gal4 target sites of a minimal promoter, thereby activating transcription from this promoter and expression of the downstream transgene. Interest in the GS was reinforced when it became clear that other regulated gene therapy constructs are compromised by severe limitations. The well-developed Tet-operon-based system proved to be immunogenic in peripheral tissues of non-human primates (NHPs), presumably due to its substantial content of bacteria-derived components.<sup>11–13</sup> Another promising system based solely on human peptide components, the rapamycin-controlled dimerizer, lacks a clinically approved alternative to the inducing drug rapamycin, which is a strong immunosuppressant and crosses the blood-brain barrier (BBB) only at a clinically unacceptable dose.<sup>14,15</sup>

We adopted the GS system for AAV vectors, aiming for a regulable expression of the neurotrophic factor GDNF as a therapeutic option to treat PD. This pre-clinical development resulted in a vector system with excellent characteristics regarding high-level inducibility, with negligible background and robust therapeutic efficacy in rodent models of PD.<sup>16–18</sup> Mfp is a US Food and Drug Administration (FDA)-approved drug and thus readily available for clinical trials, but we have found pronounced gender-specific differences in the pharmacokinetics of Mfp.<sup>18</sup> In addition, Mfp binds with high affinity to a plasma carrier protein,  $\alpha$ 1-acid glycoprotein (AAG), only in human plasma and not in rodents<sup>19,20</sup> or monkeys.<sup>21</sup> If and to which

Received 28 April 2021; accepted 30 July 2021;  
<https://doi.org/10.1016/j.omtm.2021.07.007>

<sup>3</sup>Present address: UK Dementia Research Institute, University of Cambridge, Department of Clinical Neurosciences, Hills Rd. CB2 0AH, Cambridge, UK

<sup>4</sup>Present address: Evotec, Department of in vivo Pharmacology, Marie-Curie-Strasse 7, 37079 Göttingen, Germany

**Correspondence:** Sebastian Kügler, PhD, University Medical Center Göttingen, Department of Neurology, Waldweg 33, 37073 Göttingen, Germany.

**E-mail:** [sebastian.kuegler@med.uni-goettingen.de](mailto:sebastian.kuegler@med.uni-goettingen.de)



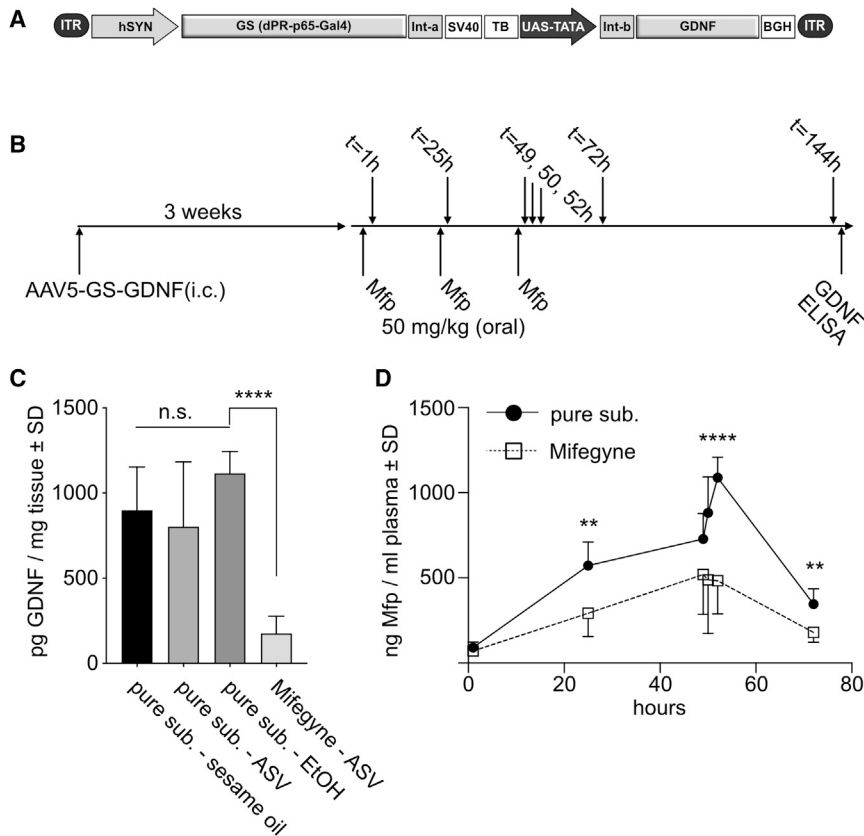


**Figure 1. Pharmacodynamics and -kinetics depending on mifepristone formulation**

(A) Schematic representation of the AAV-5-GS-GDNF vector. ITR, inverted terminal repeat from AAV-2; GDNF, glial cell line derived neurotrophic factor; WPRE, woodchuck hepatitis virus posttranscriptional regulatory element; BGH, bovine growth hormone polyadenylation site; SV40, simian virus 40 polyadenylation site; Int-a and Int-b, synthetic introns; GS, fusion protein consisting of Gal4 DNA binding domain, truncated human progesterone receptor, and human p65 transactivation domain; hSyn, 420 bp fragment of human synapsin 1 gene promoter; TB, synthetic transcription blocker; UAS-TATA, minimal TATA promoter with 6 upstream Gal4 binding sites. (B) Schematic representation of the experimental layout.  $1 \times 10^9$  vg of AAV-5-GS-GDNF was injected intracranially, and 3 weeks later Mfp was orally applied at  $3 \times 50$  mg/kg in different formulations. Plasma samples were collected at indicated time points; striatal tissue for GDNF quantification was collected at  $t = 144$  h after the first Mfp application. (C) Striatal GDNF levels obtained after oral application of various Mfp formulations. Pure sub., pure substance of Mfp; Mifegyne, tablet formulation of Mfp; Statistics by 1-way ANOVA with Dunnett's multiple comparisons test. n.s., not significant; \*\*\*\* $p < 0.0001$ ;  $n = 5$  animals per condition. (D) Plasma Mfp levels obtained at time points indicated in (A) after oral application of 50 mg/kg pure Mfp in ASV or Mifegyne in ASV. Statistics by 2-way ANOVA with Sidak's multiple comparisons test. \*\* $p < 0.01$ ; \*\*\*\* $p < 0.0001$ ;  $n = 5$  animals per condition.

extent this binding affects the transport of Mfp over the blood-brain barrier is currently unknown. Thus, a better understanding of Mfp's pharmacokinetics and -dynamics in terms of GDNF induction is urgently needed. We accomplished this in a rat model expressing the human AAG (hAAG) protein. Our data demonstrate that interaction of Mfp with hAAG did not prevent activation of the GS-GDNF vector in the brain and thus suggest that equivalent levels of GDNF can be expected to be induced in human brain as compared to the brains of experimental animals. We furthermore demonstrate that the formulation of Mfp can significantly impact its pharmacodynamic effectivity and that a clinically approved pharmacological booster, ritonavir (Rtv), enhances the effect of Mfp by an order of magnitude, both in rodents and non-human primates. As a cautionary note, our data also suggest that individual pharmacokinetics of Mfp should be taken into account for individual patients.

## RESULTS

### Different formulations of Mfp result in largely different pharmacokinetics and -dynamics

Mfp is a synthetic steroid with very low solubility in water. Thus, in our previous pre-clinical studies, we had used the compound mostly dissolved in DMSO and applied by intraperitoneal (i.p.) injection. However, oral application would be much preferred for use in patients. We therefore studied the pharmacodynamic effect of various oral formulations of Mfp on induction of GS-controlled expression

of the neurotrophic factor GDNF. To this end, 2-month-old female rats were intracranially injected with  $1 \times 10^9$  vg of AAV-5-GS-GDNF (Figure 1A), and 3 weeks later Mfp was orally applied on 3 consecutive days at 50 mg/kg (see Materials and methods for conversion into human equivalent dosages) (Figure 1B). Mfp was used as pure substance, which was either dissolved in EtOH, suspended in sesame oil, or suspended in aqueous suspension vehicle (ASV). Alternatively, Mfp was used as the commercially available Mifegyne formulation (200 mg/tablet), suspended in ASV. GDNF expression in the brain (i.e., within the striatum, into which the vector had been applied) was determined by ELISA at 4 days after the last Mfp application.

Our results demonstrate that the solvent/carrier used for oral administration had no influence on pharmacodynamics of Mfp in brain tissue, as GDNF levels obtained were very similar after dissolving Mfp in EtOH or suspending it in sesame oil or ASV. However, the source of the drug had a profound influence on its pharmacodynamics, in that the same dosage of Mifegyne, as compared to the pure substance, resulted in 5-fold less activation of the GS system as compared to the pure substance (Figure 1C). The reduced bioavailability of Mifegyne was confirmed by substantially reduced plasma Mfp levels (Figure 1D), with an area under the curve (AUC) of  $40,653 \pm 3,352$  ng/mL  $\times$  h for the pure substance, and  $22,181 \pm 4,185$  ng/mL  $\times$  h for Mifegyne.

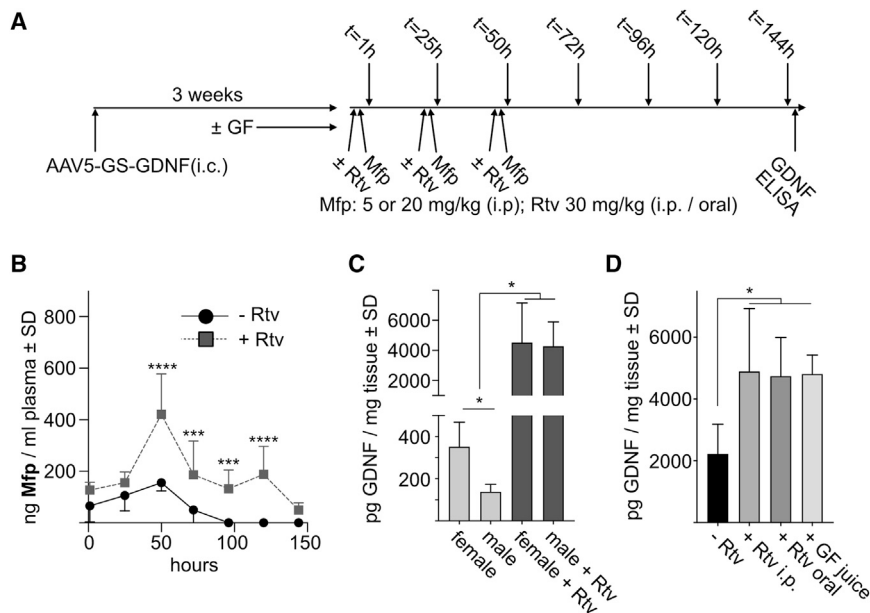


**Figure 2. Cyp3A4 inhibition by ritonavir boosts pharmacokinetics and -dynamics of Mfp**

(A) Schematic representation of the experimental layout.  $1 \times 10^9$  vg of AAV-5-GS-GDNF was injected intracranially, and 3 weeks later Mfp was applied i.p. with a co-application of Rtv 20 min before Mfp application. Plasma samples were collected at indicated time points; striatal tissue for GDNF quantification was collected at  $t = 144$  h after the first Mfp application. In some animals, grapefruit juice (GF) was given orally for 1 week before Mfp application, as an alternative Cyp3A4 inhibitor. (B) Plasma levels of Mfp in female rats after application of  $3 \times 5$  mg/kg Mfp i.p., without (black circles) and with (gray squares) Rtv co-application. Statistics by 2-way ANOVA with Sidak's multiple comparisons test. \*\*\* $p < 0.001$ ; \*\*\*\* $p < 0.0001$ ;  $n = 5$  animals per condition. (C) Striatal GDNF levels in female and male rats after application of  $3 \times 5$  mg/kg Mfp i.p., without (light gray bars) and with (dark gray bars) co-application of Rtv. Note the split Y-scale. Statistics by 1-way ANOVA with Dunnett's test for multiple comparisons. \* $p < 0.05$ ;  $n = 5$  animals per condition. (D) Striatal GDNF level in female rats after application of  $3 \times 20$  mg/kg Mfp i.p., without Rtv co-application (– Rtv), with co-application of 30 mg/kg Rtv i.p. (+ Rtv i.p.), with co-application of 30 mg/kg Rtv orally (+ Rtv oral), and with co-application of 50% grapefruit juice (+ GF juice). Statistics by 1-way ANOVA with Dunnett's test for multiple comparisons. \* $p < 0.05$ ;  $n = 3$ –5 animals per condition.

### Cyp3A4 inhibition robustly enhances the pharmacodynamic response to Mfp

We have recently reported that Mfp exerts largely different pharmacodynamics with respect to induction of GDNF expression in male versus female rats.<sup>18</sup> Thus, we sought to optimize the pharmacodynamic properties of Mfp through temporal inhibition of Cyp3A4, which is the liver cytochrome known to be primarily responsible for degradation of Mfp.<sup>22</sup> A suitable drug, which is both clinically approved for this purpose and has an excellent safety profile, was identified in Rtv, initially developed as an HIV protease inhibitor.<sup>23</sup>

In order to determine if Cyp3A4 is indeed responsible for gender-specific pharmacokinetics of Mfp and to elucidate if Cyp3A4 inhibition can prevent this effect, we applied Rtv i.p. at 30 mg/kg, 20 min before Mfp application (5 mg/kg, i.p.) on 3 consecutive days in male and female rats 2.5 months of age that had received striatal injection of AAV-5-GS-GDNF 3 weeks earlier (Figure 2A). Plasma Mfp levels were substantially elevated when Cyp3A4 activity was inhibited by Rtv, and Mfp persisted in plasma for about 2 days longer as compared to application without Cyp3A4 inhibition (Figure 2B). The AUC for plasma Mfp roughly tripled with Cyp3A4 inhibition (– Rtv =  $8,197 \pm 1,600$  ng/mL  $\times$  h; + Rtv =  $27,813 \pm 4,131$  ng/mL  $\times$  h; Figure 2B).

In both male and female rats, Rtv substantially enhanced pharmacodynamics of Mfp: both genders showed GDNF levels of about 4,000 pg/mg tissue, as compared to about 350 pg/mg GDNF in females and 100 pg/mg GDNF in male rats that received only Mfp (Figure 2C). Thus, Rtv boosted GDNF induction about 10-fold in female rats and

about 40-fold in male rats. A second group of female rats that were injected at 2 months of age with AAV-5-GS-GDNF was treated with Mfp at a higher dosage of 20 mg/kg body weight, resulting in striatal GDNF levels of about 2,000 pg/mg tissue without Rtv co-application and in striatal GDNF levels of about 4,000 pg/mg tissue after co-application of Rtv, which was given either i.p. or orally (30 mg/kg) (Figure 2D). This experiment demonstrated that the application route of Rtv does not affect its booster effect and that GDNF levels of about 4,000 pg/mg tissue are likely to represent the maximum capacity to synthesize the neurotrophic factor from the AAV-5-GS-GDNF vector at the vector titer applied in these animals. Notably, GDNF levels of about 100 pg/mg tissue have been shown to be sufficient for a neurorestorative treatment regime in the partial striatal 6-OHDA model of PD, if expressed for two relatively short intermittent intervals starting 5 weeks after the 6-OHDA lesion was induced.<sup>16</sup>

We also used a natural inhibitor of Cyp3A4, grapefruit juice,<sup>24</sup> that was given to female rats injected with AAV-5-GS-GDNF as a 50% solution in water, for 7 days before application of Mfp (20 mg/kg,  $3 \times$  i.p.). Intriguingly, grapefruit juice demonstrated the same potency in boosting Mfp pharmacodynamics as Rtv, resulting in induced striatal GDNF levels of about 4,000 pg/mg tissue (Figure 2D).

### Mfp and Rtv act cooperatively in non-human primates

We next aimed to prove the pharmacokinetic boosting effect of Rtv on Mfp plasma levels in an experimental animal model system as closely related to humans as possible (i.e., NHPs). Large animal models are

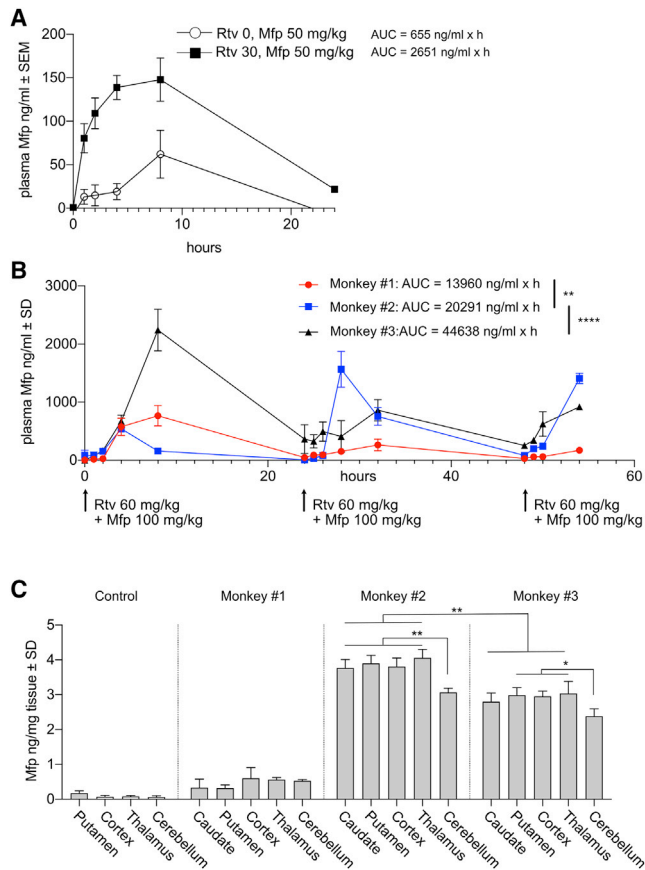


**Figure 3. Rtv/Mfp co-application in non-human primates provides brain Mfp levels sufficient for GS activation**

(A) Plasma levels of Mfp in male cynomolgus monkeys after a single oral application of 50 mg/kg Mfp alone (open circles) or co-application of 30 mg/kg Rtv with 50 mg/kg Mfp (black squares). (B) Plasma levels of Mfp after repeated oral co-application of Rtv (60 mg/kg) with Mfp (100 mg/kg) in three individual monkeys (#1, #2, #3). Statistics by unpaired Student's *t* test for pairwise comparisons of AUCs. \*\**p* < 0.01; \*\*\*\**p* < 0.0001. (C) Brain levels of Mfp after the repeated co-application scheme of Rtv and Mfp as shown in (B). Statistics by 1-way ANOVA with Tukey's test for multiple comparisons. \**p* < 0.05; \*\**p* < 0.01.

important to verify rodent-based data in animals of non-clonal origin, as only these allow us to elucidate individual responses based on individual differences in drug absorption, distribution, and metabolism. We also aimed to prove that in NHP Mfp reaches deep brain structures like the caudate/putamen (corresponding to the striatum in rodents) in relevant amounts, as a pre-requisite to any therapeutic application of GS-controlled GDNF expression in patients.

Three male cynomolgus monkeys were given 50 mg/kg Mfp with or without prior application of 30 mg/kg Rtv. Both drugs were applied through a naso-gastric probe in order to ensure optimal oral delivery. Quantification of plasma Mfp levels clearly demonstrated that in the monkeys Rtv exerted a comparable effect as in rodents (Figure 3A): without Rtv, plasma Mfp levels reached 55 ng/mL, with an AUC of 655 ng/mL × h over the 24 h of sampling. Rtv co-application

increased peak plasma levels of Mfp to 150 ng/mL, with an AUC of 2,651 ng/mL × h. However, we noted substantial variability in Mfp plasma levels in both groups (note that error bars are given as SEM instead of SD for the sake of clarity of presentation in Figure 3A), suggesting that in NHPs individual differences in drug resorption, distribution, and metabolism might be important to consider. Thus, in a second experiment we co-applied higher dosages of Rtv (60 mg/kg) and Mfp (100 mg/kg) on 3 consecutive days, hoping that this mode of application would level out individual responses. Plasma Mfp was quantified over time, and finally we quantified levels of Mfp in different brain areas (Figures 3B and 3C). Monkeys #2 and #3 showed a response, with plasma Mfp levels exceeding 500 ng/mL on all 3 days. Monkey #1, however, reached this level only at the first day of Mfp application, but not on the second and third days. Consequently, we found significantly lower Mfp levels in the brain of this monkey (Figure 3C). These findings suggest that individual differences in resorption/distribution of Mfp may cause significantly different levels of the compound in the brain. In any case, brain Mfp levels of about 0.5 ng/mg are sufficient to induce neuro-restorative levels of GDNF in rodents (see Figure 5E), and thus even the lowest level of Rtv-aided Mfp resorption/distribution seen in NHPs would be appropriate to induce therapeutically active GDNF expression.

#### AAV-GS-GDNF is fully active in animals “humanized” for plasma binding capabilities of Mfp

There is an important species-specific aspect that needs to be considered when attempting to transfer the GS from pre-clinical models to humans: only in human plasma, but not in plasma of any other species, including NHPs, Mfp is bound by a carrier protein,  $\alpha$ 1-acid glycoprotein (AAG) or orosomucoid.<sup>25</sup> Mfp-binding to hAAG significantly prolongs plasma half-life ( $T_{1/2}$  = 4 h in rats, 30 h in human) and significantly reduces clearance (2.7 L/h/kg body weight in rats, 0.04 L/h/kg body weight in human).<sup>26</sup> It is currently unknown if Mfp binding to hAAG will impact pharmacodynamics of Mfp in terms of GS-GDNF activation. On the one hand, binding of Mfp to its carrier might sequester the steroid and thus prevent it from crossing the blood-brain barrier in sufficient amounts to activate GS-GDNF. If this would be the case, higher dosages of Mfp would be necessary in humans, as was deduced from the rodent studies. On the other hand, prolonged plasma half-life of hAAG-bound Mfp might result in a longer-lasting release and delivery over the blood-brain barrier, which might also result in higher levels of GDNF induction.

As hAAG is mainly synthesized by hepatocytes and parenchymal cells in the liver,<sup>27</sup> we constructed an AAV-1/2 hybrid vector to express hAAG from a liver-specific LP1 promoter.<sup>28</sup> Intravenous application of  $1 \times 10^{12}$  vg AAV-1/2-LP1-hAAG in 2-month-old female rats resulted in sustained hAAG levels of about 0.4–0.5 mg/mL, which is reasonably comparable to levels found in healthy humans (0.4–0.6 mg/mL)<sup>29</sup> (Figures 4A and 4B).

In order to prove that hAAG-expressing rats are functional in terms of plasma Mfp binding, we applied Mfp either as a single

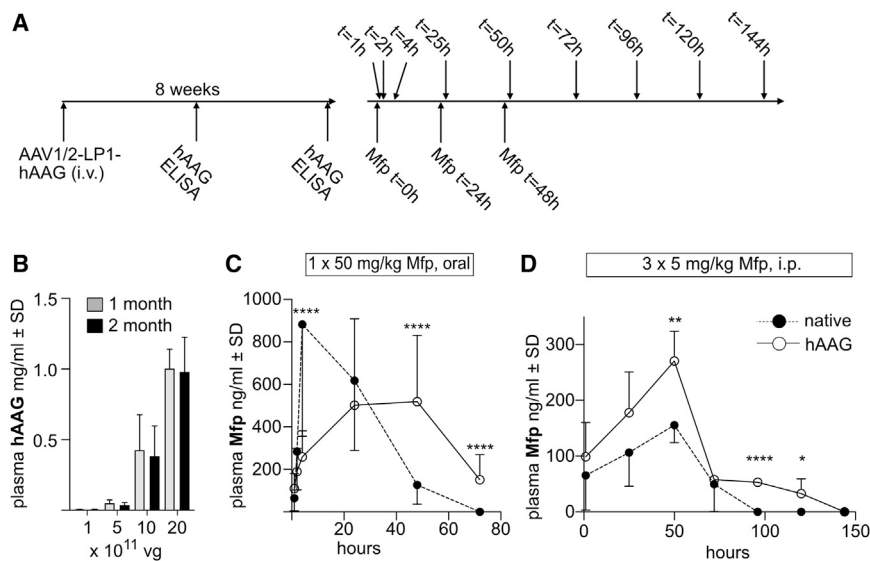


**Figure 4. Mfp plasma concentrations in hAAG-humanized rats**

(A) Schematic representation of the experimental layout. AAV-LP1-hAAG was injected intravenously, and 4 and 8 weeks later plasma levels of hAAG were determined. In animals with appropriate hAAG level, Mfp was applied either orally once at 50 mg/kg or 3× i.p. at 5 mg/kg. Plasma samples were taken at times indicated above the arrow. (B) hAAG plasma levels obtained after i.v. injection of AAV-1/2-LP1-hAAG vectors at titers of  $1 \times 10^{11}$  vg,  $5 \times 10^{11}$  vg,  $10 \times 10^{11}$  vg, and  $20 \times 10^{11}$  vg, determined at 1 month (gray bars) and 2 months (black bars) after vector application. N = 4–5 animals per condition. (C) Mfp plasma levels obtained in native (black circles) and hAAG-expressing (open circles) rats after a single oral dose of 50 mg/kg Mfp. (D) Mfp plasma levels obtained in native (black circles) and hAAG-expressing (open circles) rats after a triple i.p. dose of 5 mg/kg Mfp. Statistics by 2-way ANOVA with Sidak's multiple comparisons test. \* $p < 0.05$ ; \*\* $p < 0.01$ ; \*\*\*\* $p < 0.0001$ ; n = 13 in (C) and 10 in (D).

oral dose of 50 mg/kg or as three consecutive i.p. doses of 5 mg/kg and followed Mfp plasma levels in native and hAAG-expressing rats. These data demonstrated that in hAAG-expressing rats, Mfp persists considerably longer in plasma as compared to native rats. After a single oral dose, Mfp plasma levels increased slower in hAAG-expressing rats as compared to native rats, but while at 48 h after application in native rats plasma Mfp levels had dropped by over 80%, they were still at maximum level in hAAG-expressing rats (Figure 4C). At 72 h after oral Mfp dosage, plasma levels in hAAG-expressing rats were still at about one-third of maximum levels, while Mfp was no longer detectable in plasma of native rats. Repeated i.p. application of Mfp resulted in somewhat different plasma pharmacokinetics of Mfp as compared to oral application, in that early peak plasma levels were substantially higher in hAAG-expressing rats as compared to native rats. Again, plasma Mfp persisted significantly longer in hAAG-expressing rats, where it was clearly detectable at 96 h and 120 h after the first dosing (Figure 4D), while in native rats, plasma Mfp was no longer detectable at these times. Thus, after both application schemes, we found robustly prolonged plasma half-lives of Mfp in hAAG-expressing rats, suggesting that these animals mimic the human situation reasonably well.

In order to be able to compare results obtained in hAAG-expressing rats with those of our previous studies in native rodents, we evaluated pharmacodynamics of Mfp in terms of GS-GDNF activation by applying Mfp at  $3 \times 5$  mg/kg and  $3 \times 20$  mg/kg i.p., both in hAAG-expressing and native animals (Figure 5A). As shown in Figure 2B, application of  $3 \times 5$  mg/kg Mfp i.p. results in peak plasma levels of about 150 ng/mL, corresponding to about 0.3  $\mu$ M of Mfp. After i.p. application of  $3 \times 20$  mg/kg, we had determined peak plasma levels of about 750 ng/mL in an earlier study (see Figure 4C in Cheng et al.<sup>18</sup>), corresponding to 1.9  $\mu$ M Mfp. These concentrations are well within the range where Mfp is bound by human plasma protein to an

extent of >98%,<sup>30</sup> ensuring that the conditions applied are as similar as possible to the human situation.

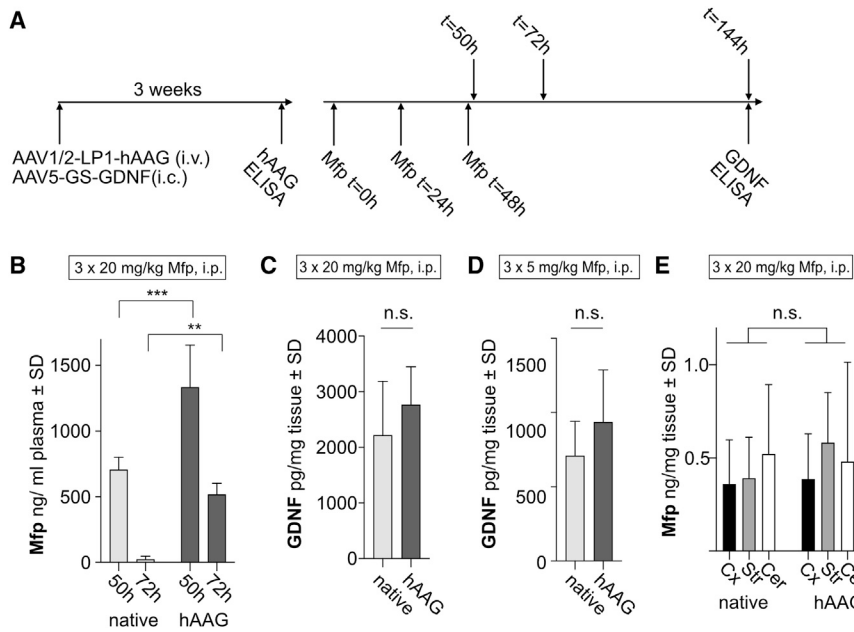
As shown in Figure 5B, plasma Mfp levels were significantly elevated at 50 h and especially at 72 h in hAAG-expressing animals as compared to native animals, after  $3 \times 20$  mg/kg Mfp. Striatal GDNF levels were similar in both animal groups, indicating that hAAG binding of Mfp did not impact its capability to cross the blood-brain barrier and to induce GS-GDNF. Using the lower dosage of  $3 \times 5$  mg/kg Mfp also showed no negative effect on GS-GDNF activation (Figure 5D), indicating that at both dosages the presence of the plasma carrier of Mfp did not influence its pharmacodynamics in terms of GS-GDNF activation. Equal GDNF levels in native and hAAG-expressing animals corresponded well with equal Mfp levels in their brain tissue (Figure 5E).

#### Aging robustly affects the pharmacodynamic effect of Mfp on the GS-GDNF vector

Finally, we addressed the effect of aging on pharmacodynamics of Mfp with respect to induction of GDNF expression in the brain. To this end, we expressed GS-GDNF in female and male rats 2 months of age and in female and male rats 15 months of age. As shown in Figure 6, induced levels of GDNF were about 7–8 times higher in aged animals as compared to young animals, in both genders. These data suggest that bioavailability of Mfp depends dramatically on the age of the subject, at least in rodents.

#### DISCUSSION

The compound used to control a regulable vector is probably the most important single player in the whole system. It must be clinically approved, devoid of side effects, preferably orally available, allow for decent induction of gene expression, and, in the case of gene therapy for brain diseases, must cross the blood-brain barrier at acceptable dosages. Furthermore, the compound should exert its



and hAAG-humanized rats (right). Mfp levels were determined at  $t = 144$  h (i.e., at the same time when GDNF levels were determined in brain tissue). Cx, cortex; Str, striatum; Cer, cerebellum. Statistics by 1-way ANOVA with Tukey's test for multiple comparisons.  $n = 5$  animals per condition.

pharmacodynamic effect over a certain range of dosages in order to allow for adjustments to individual patient's needs. While Mfp has demonstrated many of these features, considerable issues remained to be addressed. The fact that Mfp had been developed as an emergency contraceptive for younger females may explain the substantial lack of pharmacological data for males and older individuals and for CNS applications in general.

1. Origin of Mfp: while our data demonstrate that Mfp can be given in various oral formulations, they also show that the pure substance seems to be absorbed far better than the commercially available Mifegyne formulation. Thus, application of the pure substance may allow use of lower dosages or induce higher levels of GDNF in PD patients.

2. Cyp3A4 inhibition: our data unequivocally demonstrate that gender-specific pharmacokinetic differences of Mfp can be resolved by inhibition of its major degradation pathway through cytochrome P430 3A4. Furthermore, the pharmacodynamic effect of Mfp in terms of GDNF induction can be substantially boosted by Cyp3A4 inhibition through Rtv. Actually, Rtv is in clinical use mainly due to its robust inhibitory effect on Cyp3A4,<sup>31,32</sup> as an adjunct therapy for HIV protease inhibitors,<sup>33</sup> but also for treatment of hepatitis C virus infections,<sup>34</sup> with a well-acceptable safety profile. However, metabolic effects of Rtv, such as a moderate increase in insulin resistance,<sup>35</sup> should be monitored, even after the infrequent co-application of Rtv with Mfp, as considered for activation of the GS.

Side effects even after long-term daily use of high doses of Mfp, due to its binding to progesterone and glucocorticoid receptors, are only

very mild (reversible asthenia and rashes).<sup>26</sup> Human equivalent doses (HEDs) exceeding those of 50 mg/kg in rodents have been safely applied for 14 consecutive days in males,<sup>36</sup> and HEDs exceeding 20 mg/kg in rats have been safely applied to males and non-pregnant women daily for several months.<sup>37,38</sup>

For a continuous activation of GDNF production, we consider a monthly application of Mfp on 3 consecutive days to be sufficient,<sup>16,18</sup> but even in this case, co-dosage with Rtv may allow use of dosages of Mfp that are completely devoid of any potential side effects. Alternatively, Rtv may be exploited to induce maximal levels of GDNF: the dynamic range of the AAV-5-GS-GDNF vector appears to be extremely wide, reaching from zero non-induced background<sup>16,18</sup> to induced levels of about 700-fold over that of the endogenous rat brain GDNF levels of 5–6 pg/mg tissue, if Rtv is used as a booster drug. This potency of induction may be used in a way that high levels of GDNF are triggered in initial treatment stages, in order to initiate resprouting of dopaminergic innervation in the basal ganglia, while much lower levels of GDNF would be induced in later stages of treatment, in order to prevent side effects.

However, our results obtained with Cyp3A4 inhibition by grapefruit juice also suggest that care must be taken to avoid excessive levels of AAV-GS-GDNF activation by nutritional components like furanocoumarins.<sup>39</sup>

3. Individual pharmacokinetics for Mfp in NHP: the NHP data generally suggest that Rtv-boosted Mfp pharmacodynamics will also be available in patients. However, the NHP data also suggest that individual differences in Mfp pharmacokinetics and -dynamics might be important to

### Figure 5. Pharmacokinetics and -dynamics of Mfp in hAAG-humanized rats

(A) Schematic representation of the experimental layout. Simultaneously,  $1 \times 10^9$  vg of AAV-GS-GDNF was injected intracranially and  $1 \times 10^{12}$  vg AAV-LP1-hAAG was injected i.v. Three weeks later hAAG levels were confirmed and Mfp was applied 3x i.p. at either 5 mg/kg or 20 mg/kg at the indicated times. Plasma samples were taken at times indicated above the arrow. (B) Plasma levels of Mfp after application of  $3 \times 20$  mg/kg, in native (light gray bars) and hAAG-humanized rats (dark gray bars). For this experiment, plasma samples were taken only at 50 h and 72 h. Statistics by 1-way ANOVA with Sidak's test for multiple comparisons. \*\* $p < 0.01$ ; \*\*\* $p < 0.001$ ;  $n = 6$  animals per condition. (C) Striatal GDNF levels after application of  $3 \times 20$  mg/kg Mfp, in native (light gray bars) and hAAG-humanized rats (dark gray bars). Statistics by two-tailed, unpaired t test. n.s., not significant.  $N = 5$  animals per condition. (D) Striatal GDNF levels after application of  $3 \times 5$  mg/kg Mfp, in native (light gray bars) and hAAG-humanized rats (dark gray bars). Statistics by two-tailed, unpaired t test. n.s., not significant.  $n = 3$  animals per condition. (E) Brain tissue levels of Mfp after application of  $3 \times 20$  mg/kg, i.p., in native animals (left)

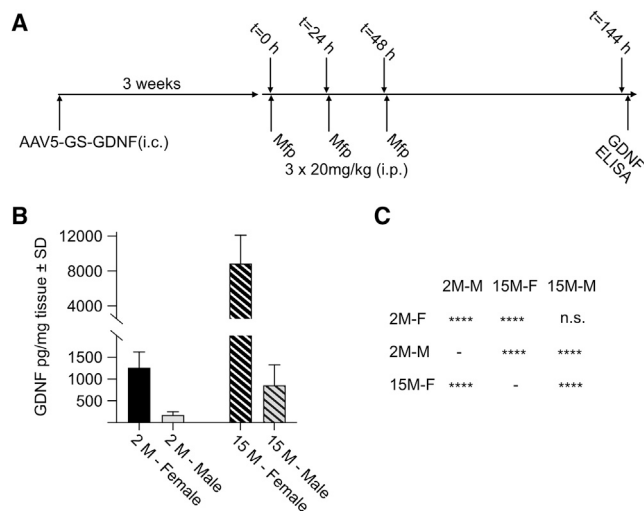


**Figure 6. Impact of aging on pharmacodynamics of Mfp**

(A) Schematic representation of the experimental layout.  $1 \times 10^9$  vg of AAV-5-GS-GDNF were injected intracranially, and 3 weeks later Mfp was applied i.p. at  $3 \times 20$  mg/kg. Striatal tissue for GDNF quantification was collected at  $t = 144$  h. (B) Striatal GDNF levels in young female and male rats 2 months of age (solid bars) and in aged female and male rats 15 months of age (hatched bars). Note the split Y-scale. (C) Statistical evaluation by 1-way ANOVA with Tukey's test for multiple comparisons. n.s. = not significant; \*\*\*\* $p < 0.0001$ ;  $n = 7$  animals each 2 months of age, and 4 animals each 15 months of age.

consider. Despite the small group size, substantially different levels of Mfp were achieved in the brain of monkey #1 versus brains of monkeys #2 and #3. While the repeated application scheme seems to level some of the different individual responses to Mfp dosage, a 6- to 7-fold difference in brain Mfp levels after the same dosage cannot be neglected. Thus, it may be advisable to determine a basic pharmacokinetic for Mfp in individual patients before treating them with the AAV-GS-GDNF vector, in order to ensure induction of similar levels of GDNF.

4. Human-specific interaction of Mfp with  $\alpha 1$ -acid glycoprotein: hAAG (also called orosomucoid) is expressed in humans by two closely related genes, ORM1 and ORM2, which, due to polymorphisms, give rise to several alleles that differ significantly in their capabilities to bind Mfp. In general, ORM2-derived AAG variants bind Mfp only weakly, while some ORM1-derived variants (ORM1F1 and ORM1S) are able to bind Mfp with high affinity, and others (ORM1F2) have only low affinity.<sup>25,40,41</sup> No gender-related differences in the ORM genes are known.<sup>42</sup> For our study, we expressed the S-variant of hAAG (arginine at amino acid position 20 and valine at amino acid position 156). While this variant alone does not represent the full spectrum of possible interactions of Mfp with human plasma carrier proteins, it can be considered representative for the high-affinity interaction of hAAG with Mfp. From our data, we conclude that there are no principal hurdles for the application of Mfp to tightly control GDNF expression from the GS vector in patients, given that in the absence and presence of hAAG the induced GDNF levels were almost identical.

5. Aging: the robust impact of aging on pharmacodynamics of Mfp might be interpreted in two controversial ways: on the one hand, this fact can be interpreted as favorable, since it can be anticipated that for the aged parkinsonian patients to be treated by gene therapy with AAV-GS-GDNF, even lower dosages of Mfp (alone or in combination with Rtv) may be used, thereby bypassing any risk of side effects caused by application of these drugs. On the other hand, it appears to be necessary to pre-screen putative recipients of this therapy for their Mfp plasma (or probably cerebrospinal fluid) levels after application of oral dosages, as was already suggested by the evident variability of Mfp pharmacokinetics in non-human primates.

It is not trivial to define a reason for the substantial effect of age on Mfp pharmacodynamics, and it is currently uncertain if it can be fully translated to the human situation. For aged rodents, a significant reduction of Cyp3A (but not specifically Cyp3A4) has been reported,<sup>43</sup> which may at least partially explain the much higher levels of GDNF induced in aged rats. However, in human liver microsomes, Cyp3A4 activity was not affected by aging<sup>44,45</sup> and thus may not impact Mfp pharmacokinetics. Nonetheless, aged individuals present with significant alterations in hepatic size and blood flow, an increased distribution volume for lipophilic drugs like Mfp in fat tissue, a generally increased interindividual variability in drug disposition,<sup>45</sup> and probably also with a less-restrictive blood-brain barrier, all of which might impact Mfp pharmacokinetics and -dynamics. Moreover, turnover rates of GDNF in brain tissue may be influenced by aging. As such, definition of human dosages of Mfp for a fine-tuned activation of the GS will likely need to take such individual parameters into account.

## MATERIALS AND METHODS

### Viral vectors

The recombinant AAV-5 vector expressing the GS under control of the neuron-specific synapsin 1 gene promoter and GDNF from the inducible UAS-TATA promoter (Figure 1A) has been described in detail elsewhere.<sup>16,18</sup> The AAV-1/2-LP1-hAAG vector expressing hAAG uses a liver-specific LP1 promoter<sup>28</sup> to express the high-affinity S-variant of hAAG,<sup>40,46</sup> which binds Mfp specifically in human plasma.<sup>25</sup> The vector was packaged into a hybrid AAV-1/2 capsid for enhanced liver tropism.<sup>47</sup> Of note, vectors exploiting a chicken-beta actin promoter or an AAV-8 capsid did not succeed in long-term expression of hAAG in rats, probably due to immunological clearance of transduced cells. Vectors were packaged in transiently transfected HEK293 cells and purified from cell lysates by iodixanol gradient ultracentrifugation and fast protein liquid chromatography (FPLC) heparin (AAV-1/2) or AVB Sepharose (AAV-5) affinity chromatography.

### Animal surgery

All animal experiments were conducted according to approved experimental animal licenses (16/2074 and 19/3117) issued by the responsible animal welfare authority (Niedersächsisches Landesamt für Verbraucherschutz und Lebensmittelsicherheit, LAVES) and controlled by the local animal welfare committee and veterinarians of University

Medical Center Göttingen and Charles River Laboratories Germany, Göttingen.

Stereotaxic injection of the AAV-5-GS-GDNF vector into the left striatum of Wistar rats was performed under ketamine/xylazine anesthesia exactly as described.<sup>16</sup> AAV-1/2-LP1-hAAG was injected intravenously (i.v.) through the tail vein at times of intracranial injection of AAV-5-GS-GDNF. Blood samples of about 250  $\mu$ L were collected from the tail vein into KE3 type Sarstedt tubes including 1.6 mg EDTA/mL, centrifuged for 10 min at 4°C and 10,000 rpm, and plasma was stored at –20°C until use. Mfp and Rtv were applied orally by gavage or injected i.p. in volumes of 1 mL/kg body weight.

Three experimentally non-naive, male cynomolgus macaques (*Macaca fascicularis*) of Chinese origin, aged 3–4 years were used for NHP experiments. Animals were group-housed in group cages in a climate-controlled room with a 12-h light 12-h dark cycle. The temperature and relative humidity ranges were 22.5°C–25.5°C and 40%–70%, respectively. Water was available *ad libitum*. Animals were provided daily with sufficient meals of balanced composition providing sufficient gross nutrients. In addition, fresh fruit or vegetables were provided daily as a food supplement.

Mfp (t = 0) and Rtv (t = –1 h) were applied orally using a nasogastric tube (10 mL per compound) at a single dose (Mfp: 50 mg/kg, Rtv: 30 mg/kg), or a repeated dose (Mfp: 100 mg/kg, Rtv: 60 mg/kg, once daily for 3 days), as described in Figure 3. Due to training in previous experiments, the animals were used to sitting in a subject chair for the duration of the experiment, so that blood sampling and application of the substances could be done without anesthesia. Finally, animals were anaesthetized by intramuscular (i.m.) application of ketamine (10 mg/kg), and xylazine (0.05 mg/kg) and sacrificed by a pentobarbital overdose (>50 mg/mL) i.v. Animals were intracardially perfused with ice-cold PBS, and the brain was removed for analysis.

### Drugs

Mfp was obtained as pure substance from Sigma (M8046) or as tablet formulation Mifegyne (200 mg/tablet; Mfp content confirmed by high-performance liquid chromatography [HPLC] with diode array detection, see below) from Nordic Pharma. Rtv was obtained from AbbVie as Norvir 100 mg. Mfp and Rtv were either diluted in DMSO for i.p. application or suspended in ASV (0.9% NaCl [w/v], 0.5% carboxymethyl-cellulose MW 250,000 [w/v], 0.4% polysorbate 80 [v/v], 0.9% benzyl alcohol [v/v]). Mfp was also used as suspension in sesame oil.

Drug dosages applied to rats and monkeys can be converted to HEDs according to the FDA-approved body surface area (BSA) normalization approach.<sup>48,49</sup> Specifically, calculating  $HED(mg/kg) = animal\ dose(mg/kg) \times (animal\ weight\ kg / human\ weight\ kg)^{1-0.67}$  results in the following conversion factors: for rats weighing 250 g, monkeys weighing 3 kg, and an assumed human weight of 70 kg: rat dosage (e.g., 50 mg/kg)  $\times$  0.156 = HED (7.8 mg/kg); monkey dosage (e.g., 50 mg/kg)  $\times$  0.357 = HED (17.9 mg/kg). In addition,

it must be considered that bioavailability of Mfp in monkeys (15%) is considerably lower compared to humans and rats (40%),<sup>19</sup> justifying higher dosages to be applied in monkeys as compared to rats.

### hAAG and GDNF ELISAs

For quantification of hAAG levels in plasma samples, the hAAG ELISA R&D DY3694 was used exactly as specified by the manufacturer. Quantification of striatal GDNF levels was performed essentially as described.<sup>16</sup>

### Quantification of Mfp from plasma and tissue samples

Quantification of Mfp from plasma samples was performed by HPLC on an Ultimate 3000 system equipped with C18-RP column (5  $\mu$ m, 120 Å, 2.1  $\times$  250 mm, mobile phase 25% methanol, 47% acetonitrile, 28% water) and diode array detection (304 nm for Mfp, 254 nm for the internal standard loratadine) or ISQ EC single quadrupole mass spectrometry detection. For liquid-liquid extraction, a 50  $\mu$ L plasma sample was mixed with 5  $\mu$ L 10% acetic acid, 100  $\mu$ L methanol, 5  $\mu$ L 1 mg/mL loratadine, and 1 mL ethyl acetate. After vortexing for 20 s and centrifugation at 10,000 rpm for 5 min at room temperature (RT), the supernatant was transferred to a new tube. The pellet was reextracted with the same procedure and the combined supernatants dried down under vacuum. The sample was reconstituted in 50  $\mu$ L methanol and loaded onto the HPLC.

Tissue samples were snap frozen on dry ice, then lysed by mechanical disruption with 1.4 mm zirconium beads in a Precellys tissue homogenizer in the same organic extraction solution as described for plasma samples.

### ACKNOWLEDGMENTS

We are grateful to Monika Zebski and Sonja Heyroth for expert technical assistance and to Dr. Mylène Divivier for help with the NHP study. Shi Cheng received a fellowship from the Overseas Study Program of the Guangzhou Elite project.

### AUTHOR CONTRIBUTIONS

S.C.: investigation, methodology, formal analysis, validation, and visualization; M.M.v.G.: conceptualization and project administration; M.B.: resources; E.G.-R.: investigation, methodology, project administration, and supervision; S.K.: conceptualization, methodology, formal analysis, validation, visualization, supervision, and writing the manuscript.

### DECLARATION OF INTERESTS

M.M.v.G. and E.G.-R. are employees of Charles River Laboratories. M.M.v.G. owns stocks from Charles River Laboratories. All other authors declare no competing interests.

### REFERENCES

1. Kordower, J.H., Olanow, C.W., Dodiya, H.B., Chu, Y., Beach, T.G., Adler, C.H., Halliday, G.M., and Bartus, R.T. (2013). Disease duration and the integrity of the nigrostriatal system in Parkinson's disease. *Brain* 136, 2419–2431.

2. Arvidsson, A., Kirik, D., Lundberg, C., Mandel, R.J., Andberg, G., Kokaia, Z., and Lindvall, O. (2003). Elevated GDNF levels following viral vector-mediated gene transfer can increase neuronal death after stroke in rats. *Neurobiol. Dis.* 14, 542–556.
3. Georgievska, B., Kirik, D., and Björklund, A. (2002). Aberrant sprouting and down-regulation of tyrosine hydroxylase in lesioned nigrostriatal dopamine neurons induced by long-lasting overexpression of glial cell line derived neurotrophic factor in the striatum by lentiviral gene transfer. *Exp. Neurol.* 177, 461–474.
4. Domanskyi, A., Saarma, M., and Airavaara, M. (2015). Prospects of Neurotrophic Factors for Parkinson's Disease: Comparison of Protein and Gene Therapy. *Hum. Gene Ther.* 26, 550–559.
5. Kügler, S. Pharmacologically controlled neurotrophic factor gene therapy for Parkinson's disease. (2018). In M. Li and B. Snider, eds. *Gene therapy in neurological disorders* (Academic Press), pp. 177–193.
6. Wang, Y., O'Malley, B.W., Jr., Tsai, S.Y., and O'Malley, B.W. (1994). A regulatory system for use in gene transfer. *Proc. Natl. Acad. Sci. USA* 91, 8180–8184.
7. Wang, Y., DeMayo, F.J., Tsai, S.Y., and O'Malley, B.W. (1997). Ligand-inducible and liver-specific target gene expression in transgenic mice. *Nat. Biotechnol.* 15, 239–243.
8. Burcin, M.M., Schiedner, G., Kochanek, S., Tsai, S.Y., and O'Malley, B.W. (1999). Adenovirus-mediated regulable target gene expression in vivo. *Proc. Natl. Acad. Sci. USA* 96, 355–360.
9. Oligino, T., Poliani, P.L., Wang, Y., Tsai, S.Y., O'Malley, B.W., Fink, D.J., and Glorioso, J.C. (1998). Drug inducible transgene expression in brain using a herpes simplex virus vector. *Gene Ther.* 5, 491–496.
10. Ye, X., Schillinger, K., Burcin, M.M., Tsai, S.Y., and O'Malley, B.W. (2002). Ligand-inducible transgene regulation for gene therapy. *Methods Enzymol.* 346, 551–561.
11. Favre, D., Blouin, V., Provost, N., Spisek, R., Porrot, F., Bohl, D., Marmé, F., Chérel, Y., Salvetti, A., Hurtrel, B., et al. (2002). Lack of an immune response against the tetracycline-dependent transactivator correlates with long-term doxycycline-regulated transgene expression in nonhuman primates after intramuscular injection of recombinant adeno-associated virus. *J. Virol.* 76, 11605–11611.
12. Stieger, K., Le Meur, G., Lasne, F., Weber, M., Deschamps, J.Y., Nivard, D., Mendes-Madeira, A., Provost, N., Martin, L., Moullier, P., and Rolling, F. (2006). Long-term doxycycline-regulated transgene expression in the retina of nonhuman primates following subretinal injection of recombinant AAV vectors. *Mol. Ther.* 13, 967–975.
13. Le Guiner, C., Stieger, K., Toromanoff, A., Guilbaud, M., Mendes-Madeira, A., Devaux, M., Guigand, L., Chérel, Y., Moullier, P., Rolling, F., and Adjali, O. (2014). Transgene regulation using the tetracycline-inducible TetR-KRAB system after AAV-mediated gene transfer in rodents and nonhuman primates. *PLoS ONE* 9, e102538.
14. Rivera, V.M., Gao, G.P., Grant, R.L., Schnell, M.A., Zoltick, P.W., Rozamus, L.W., Clackson, T., and Wilson, J.M. (2005). Long-term pharmacologically regulated expression of erythropoietin in primates following AAV-mediated gene transfer. *Blood* 105, 1424–1430.
15. Hadaczek, P., Beyer, J., Kells, A., Narrow, W., Bowers, W., Federoff, H.J., Forsayeth, J., and Bankiewicz, K.S. (2011). Evaluation of an AAV2-based rapamycin-regulated glial cell line-derived neurotrophic factor (GDNF) expression vector system. *PLoS ONE* 6, e27728.
16. Tereshchenko, J., Maddalena, A., Bähr, M., and Kügler, S. (2014). Pharmacologically controlled, discontinuous GDNF gene therapy restores motor function in a rat model of Parkinson's disease. *Neurobiol. Dis.* 65, 35–42.
17. Maddalena, A., Tereshchenko, J., Bähr, M., and Kügler, S. (2013). Adeno-associated Virus-mediated, Mifepristone-regulated Transgene Expression in the Brain. *Mol. Ther. Nucleic Acids* 2, e106.
18. Cheng, S., Tereshchenko, J., Zimmer, V., Vachey, G., Pythoud, C., Rey, M., Liefhebber, J., Raina, A., Streit, F., Mazur, A., et al. (2018). Therapeutic efficacy of regulable GDNF expression for Huntington's and Parkinson's disease by a high-induction, background-free "GeneSwitch" vector. *Exp. Neurol.* 309, 79–90.
19. Deraedt, R., Bonnat, C., Busigny, M., Chatelet, P., Cousty, C., Mouren, M., Philibert, D., Pottier, J., and Salmon, J. (1985). Pharmacokinetics of RU 486. In *The Antiprogesterin Steroid RU 486 and Human Fertility Control*, E. Baulieu and S. Segal, eds. (Plenum Press), pp. 103–122.
20. Moguilewsky, M., and Philibert, D. (1985). Biochemical profile of RU 486. In *The Antiprogesterin Steroid RU 486 and Human Fertility Control*, E. Baulieu and S. Segal, eds. (Plenum Press), pp. 87–97.
21. Lerner, J.M., Reel, J.R., and Blye, R.P. (2000). Circulating concentrations of the anti-progestins CDB-2914 and mifepristone in the female rhesus monkey following various routes of administration. *Hum. Reprod.* 15, 1100–1106.
22. Jang, G.R., Wrighton, S.A., and Benet, L.Z. (1996). Identification of CYP3A4 as the principal enzyme catalyzing mifepristone (RU 486) oxidation in human liver microsomes. *Biochem. Pharmacol.* 52, 753–761.
23. Deeks, S.G., Smith, M., Holodniy, M., and Kahn, J.O. (1997). HIV-1 protease inhibitors. A review for clinicians. *JAMA* 277, 145–153.
24. Bailey, D.G., Malcolm, J., Arnold, O., and Spence, J.D. (1998). Grapefruit juice-drug interactions. *Br. J. Clin. Pharmacol.* 46, 101–110.
25. Israili, Z.H., and Dayton, P.G. (2001). Human alpha-1-glycoprotein and its interactions with drugs. *Drug Metab. Rev.* 33, 161–235.
26. Sitruk-Ware, R., and Spitz, I.M. (2003). Pharmacological properties of mifepristone: toxicology and safety in animal and human studies. *Contraception* 68, 409–420.
27. Berger, E.G., Alpert, E., Schmid, K., and Isselbacher, K.J. (1977). Immunohistochemical localization of alpha-1-acid-glycoprotein in human liver parenchymal cells. *Histochemistry* 51, 293–296.
28. Graham, T., McIntosh, J., Work, L.M., Nathwani, A., and Baker, A.H. (2008). Performance of AAV8 vectors expressing human factor IX from a hepatic-selective promoter following intravenous injection into rats. *Genet. Vaccines Ther.* 6, 9.
29. Yost, R.L., and DeVane, C.L. (1985). Diurnal variation of alpha 1-acid glycoprotein concentration in normal volunteers. *J. Pharm. Sci.* 74, 777–779.
30. Heikinheimo, O., Lähteenmäki, P.L., Koivunen, E., Shoupe, D., Croxatto, H., Luukkainen, T., and Lähteenmäki, P. (1987). Metabolism and serum binding of RU 486 in women after various single doses. *Hum. Reprod.* 2, 379–385.
31. Eagling, V.A., Back, D.J., and Barry, M.G. (1997). Differential inhibition of cytochrome P450 isoforms by the protease inhibitors, ritonavir, saquinavir and indinavir. *Br. J. Clin. Pharmacol.* 44, 190–194.
32. Greenblatt, D.J., and Harmatz, J.S. (2015). Ritonavir is the best alternative to ketoconazole as an index inhibitor of cytochrome P450-3A in drug-drug interaction studies. *Br. J. Clin. Pharmacol.* 80, 342–350.
33. Hull, M.W., and Montaner, J.S. (2011). Ritonavir-boosted protease inhibitors in HIV therapy. *Ann. Med.* 43, 375–388.
34. Brayer, S.W., and Reddy, K.R. (2015). Ritonavir-boosted protease inhibitor based therapy: a new strategy in chronic hepatitis C therapy. *Expert Rev. Gastroenterol. Hepatol.* 9, 547–558.
35. Lee, G.A., Rao, M., Mulligan, K., Lo, J.C., Aweeka, F., Schwarz, J.M., Schambelan, M., and Grunfeld, C. (2007). Effects of ritonavir and amprenavir on insulin sensitivity in healthy volunteers. *AIDS* 21, 2183–2190.
36. Donoghue, K., Rose, A., Coulton, S., Coleman, R., Milward, J., Philips, T., Drummond, C., and Little, H. (2020). Double-blind, placebo-controlled trial of mifepristone on cognition and depression in alcohol dependence. *Trials* 21, 796.
37. Perrault, D., Eisenhauer, E.A., Pritchard, K.I., Panasci, L., Norris, B., Vandenberg, T., and Fisher, B. (1996). Phase II study of the progesterone antagonist mifepristone in patients with untreated metastatic breast carcinoma: a National Cancer Institute of Canada Clinical Trials Group study. *J. Clin. Oncol.* 14, 2709–2712.
38. Grunberg, S.M., Weiss, M.H., Spitz, I.M., Ahmadi, J., Sadun, A., Russell, C.A., Lucci, L., and Stevenson, L.L. (1991). Treatment of unresectable meningiomas with the anti-progesterone agent mifepristone. *J. Neurosurg.* 74, 861–866.
39. Hung, W.L., Suh, J.H., and Wang, Y. (2017). Chemistry and health effects of furanocoumarins in grapefruit. *Yao Wu Shi Pin Fen Xi* 25, 71–83.
40. Eap, C.B., and Baumann, P. (1989). The genetic polymorphism of human alpha 1-acid glycoprotein. *Prog. Clin. Biol. Res.* 300, 111–125.
41. Hervé, F., Duché, J.C., d'Athis, P., Marché, C., Barré, J., and Tillement, J.P. (1996). Binding of disopyramide, methadone, diprydamole, chlorpromazine, lignocaine and progesterone to the two main genetic variants of human alpha 1-acid glycoprotein: evidence for drug-binding differences between the variants and for the presence

- of two separate drug-binding sites on alpha 1-acid glycoprotein. *Pharmacogenetics* 6, 403–415.
42. Duché, J.C., Hervé, F., and Tillement, J.P. (1998). Study of the expression of the genetic variants of human alpha1-acid glycoprotein in healthy subjects using isoelectric focusing and immunoblotting. *J. Chromatogr. B Biomed. Sci. Appl.* 715, 103–109.
  43. Warrington, J.S., Greenblatt, D.J., and von Moltke, L.L. (2004). Age-related differences in CYP3A expression and activity in the rat liver, intestine, and kidney. *J. Pharmacol. Exp. Ther.* 309, 720–729.
  44. Parkinson, A., Mudra, D.R., Johnson, C., Dwyer, A., and Carroll, K.M. (2004). The effects of gender, age, ethnicity, and liver cirrhosis on cytochrome P450 enzyme activity in human liver microsomes and inducibility in cultured human hepatocytes. *Toxicol. Appl. Pharmacol.* 199, 193–209.
  45. Klotz, U. (2009). Pharmacokinetics and drug metabolism in the elderly. *Drug Metab. Rev.* 41, 67–76.
  46. Fournier, T., Medjoubi-N, N., and Porquet, D. (2000). Alpha-1-acid glycoprotein. *Biochim. Biophys. Acta* 1482, 157–171.
  47. Kügler, S., Hahnewald, R., Garrido, M., and Reiss, J. (2007). Long-term rescue of a lethal inherited disease by adeno-associated virus-mediated gene transfer in a mouse model of molybdenum-cofactor deficiency. *Am. J. Hum. Genet.* 80, 291–297.
  48. US Food and Drug Administration (2005). Estimating the maximum safe starting dose in initial clinical trials for therapeutics in adult healthy volunteers, <https://www.fda.gov/media/72309/download>.
  49. Nair, A.B., and Jacob, S. (2016). A simple practice guide for dose conversion between animals and human. *J. Basic Clin. Pharm.* 7, 27–31.